Hydrogen-Bonded Layers of Hydrogen Malate Anions: A Framework for Crystal Engineering

Christer B. Aakeröy* and Mark Nieuwenhuyzen

Contribution from the School of Chemistry, David Keir Building, The Queen's University of Belfast, Belfast BT9 5AG, Northern Ireland

Received May 13, 1994. Revised Manuscript Received September 8, 1994[⊗]

Abstract: The syntheses and crystal structures of 3-hydroxy-6-methylpyridinium hydrogen L-malate (**1**), benzimidazolium hydrogen L-malate (**2**), 3-hydroxypyridinium hydrogen L-malate (**3**), and (2-chlorobenzyl)ammonium hydrogen L-malate (**4**) are described. In every case, the anions create infinite layers through two intermolecular O−H···O hydrogen bonds. In **1** and **3**, the cations provide a cross-link between adjacent anionic layers, whereas in **2** and **4**, the cations are hydrogen bonded to chains within the same layer. Despite the structural and chemical differences between the cations and the way in which they are attached to the anions, the infinite layer prevails in each compound. This illustrates that hydrogen L-malate anions may be utilized in crystal engineering as a dependable building block, "scaffolding", for two-dimensional structural frameworks in the solid state. The importance of the selectivity and directionality of the hydrogen bonds, and the influence of the cations on the geometry of individual anions and of the detailed crystal packing within these structures, is also discussed.

Introduction

The intentional design and synthesis of specific structural aggregates in the solid state, crystal engineering, continue to attract considerable academic and commercial attention,[1] since a successful incorporation of desirable structural units into a crystal may result in the development of novel materials with *cf.* improved electrical, optical, or catalytic properties. Unfortunately, the task of controlling the assembly and orientation of individual molecules into one, two, and finally three-dimensional architectures is extremely difficult, as they are capable of adopting a vast number of conformations in the crystal. However, despite such complications, important progress has been made in this area during the last few years. Halogen−halogen interactions[2] have been employed as steering forces in structures of some fluorocoumarines,[3] cocrystals of melamines and barbiturates have been used to create a variety of structural motifs,[4] and rigid aromatic spacers have provided a predictable backbone for several, well-organized, extended structures.[5,6]

Hydrogen bonding, which plays a fundamental role in the structure of DNA, and in the secondary and tertiary structure of proteins, is also responsible for some of the anomalous properties of many important compounds, *e.g.* water, ammonia, and hydrogen fluoride. Hydrogen bonding also exercises important effects on the organization and properties of many solid-state materials, *e.g.* the structure of clathrates,[7] the ferroelectricity of potassium dihydrogen phosphate,[8] and the room-temperature proton conductivity of uranyl phosphate.[9] The selectivity and directionality of the hydrogen bond have also been instrumental in the preparation of a variety of distinctive and predictable structural aggregates,[10] notably in molecular solids, and the use of hydrogen bonding as a steering force is now beginning to emerge as the most important strategy in crystal engineering. In spite of this progress, there is a paucity of studies concerned with the design of ionic materials, partly because hydrogen bonding is not always perceived to be strong enough to control the packing of ions in the solid state. However, both experimental[11] and theoretical[12] studies of hydrogen-bond strengths between ionic species indicate that the overall energetic contribution from a collection of hydrogen bonds would, in many cases, be sufficient to control the way in which ions arrange themselves in the solid state.[13] From an applications perspective (*e.g.*, thermal stability, mechanical robustness, *etc.*), ionic materials often demonstrate considerable advantages over molecular solids and may therefore, in some cases, be better suited for incorporation into working devices.

Hydrogen-bonded anionic structures, *e.g.* hydrogen tartrates,[14,15,16] dihydrogen phosphates,[17] and hydrogen sulfates,[18] have recently been shown to provide suitable "scaffolding" for

[⊗] Abstract published in *Advance ACS Abstracts*, October 15, 1994.

(1) Desiraju, G. R. *Crystal Engineering: The Design of Organic Solids*; Elsevier: Amsterdam, 1989. Lehn, J.-M. *Angew. Chem., Int. Ed. Engl.* **1990**, *29*, 1304. Mathias, J. P.; Stoddart, J. F. *Chem. Soc. Rev.* **1992**, *21*, 215. Aakeröy, C. B.; Seddon, K. R. *Chem. Soc. Rev.* **1993**, *22*, 397.

(2) Desiraju, G. R.; Parthasarathy, R. *J. Am. Chem. Soc.* **1989**, *111*, 8725.

(3) Kumar, V. A.; Begum, N. S.; Venkatesan, K. *J. Chem. Soc., Perkin Trans. 2* **1993**, 463.

(4) Zerkowski, J. A.; Whitesides, G. M. *J. Am. Chem. Soc.* **1994**, *116*, 4298.

(5) Simard, M.; Su, D.; Wuest, J. D. *J. Am. Chem. Soc.* **1991**, *113*, 4696.

(6) Garcia-Tellado, F.; Geib, S. J.; Goswami, S.; Hamilton, A. D. *J. Am. Chem. Soc.* **1991**, *113*, 9265.

(7) Vögtle, F. *Supramolecular Chemistry*; Wiley: Chichester, U.K., 1991.

(8) Lines, M. E.; Glass, A. M. *Principles and Applications of Ferroelectrics and Related Materials*; Clarendon Press: Oxford, U.K., 1979.

(9) Morosin, B. *Acta Crystallogr.* **1978**, *B34*, 3732.

(10) (a) Seto, C. T.; Whitesides, G. M. *J. Am. Chem. Soc.* **1991**, *113*, 9025. (b) Zhao, X.; Chang, Y.-L.; Fowler, F. W.; Lauher, J. W. *J. Am. Chem. Soc.* **1990**, *112*, 6627. (c) Weber, E.; Finge, S.; Csöregh, I. *J. Org. Chem.* **1991**, *56*, 7281. (d) Lehn, J.-M.; Mascal, M.; DeCian, A.; Fischer, J. *J. Chem. Soc., Perkin Trans. 2* **1992**, 461. (e) Subramanian, S.; Zaworotko, M. J. *Can. J. Chem.* **1992**, *71*, 433.

(11) Meot-Ner (Mautner), M. In *Molecular Structure and Energetics*; Liebman, J. F., Greenberg, A., Eds.; VCH Verlag: New York, 1987; Vol. 4.

(12) Deakyne, C. A. In *Molecular Structure and Energetics*; Liebman, J. F., Greenberg, A., Eds.; VCH Verlag: New York, 1987; Vol. 4.

(13) Aakeröy, C. B.; Leslie, M.; Seddon, K. R. *Struct. Chem.* **1992**, *3*, 62.

(14) Aakeröy, C. B.; Hitchcock, P. B. *J. Mater. Chem.* **1993**, *3*, 1129.

(15) Aakeröy, C. B.; Hitchcock, P. B.; Seddon, K. R. *J. Chem. Soc., Chem. Commun.* **1992**, 553.

(16) (a) Zyss, J; Pecaut, J.; Levy, J. P.; Masse, R. *Acta Crystallogr.* **1993**, *B49*, 334. (b) Dastidar, P.; Row, T. N. G.; Prasad, B. R.; Subramanian, C. K.; Bhattacharya, S. *J. Chem. Soc., Perkin Trans. 2* **1993**, *12*, 2419. (c) Bhattacharaya, S.; Dastidar, P.; Row, T. N. G. *Chem. Mater.* **1994**, *6*, 531. (d) Watanabe, O.; Noritake, T.; Hirose, Y.; Okada, A.; Kurauchi, T. *J. Mater. Chem.* **1993**, *23*, 321.

0002-7863/94/1516-10983$04.50/0

polarizable cations in novel materials for nonlinear optics. Typically, the cation is incorporated between chains, or layers, of anions held together by hydrogen bonds, and the role of such anionic aggregates has been to provide structural stability and some influence over the packing of the anions. However, detailed control over the assembly and arrangement of ions in a solid material still proves to be an elusive goal and further work is required in order to increase the choice of reliable two-dimensional building blocks and, more importantly, to allow us to rationalize and predict structural arrangements of the ions ("subunits") within such materials.

Rationale. The packing modes and hydrogen-bond preferences displayed by both carboxylic and dicarboxylic acids have been studied extensively.[19] Indeed, one of the most easily recognizable hydrogen-bond motifs is the cyclic, head-to-head, dimeric arrangement displayed by most carboxylic acids in the solid state. Furthermore, there is considerable structural evidence which shows that the most common, extended, hydrogen-bond motif in dicarboxylic acids is an infinite chain *e.g.* terephthalic acid,[20] chlorosuccinic acid,[21] and adipic acid.[22] In moving from dicarboxylic acids to monovalent dicarboxylates, some important differences in packing and hydrogen bonding become apparent; most significantly, the cyclic motif, $R_2^2(8)$,[23] has been destroyed. However, in accordance with the rule-of-thumb observed by Etter[24] which states that the best hydrogen-bond donor will form a hydrogen bond with the best hydrogen-bond acceptor, monovalent dicarboxylates also form infinite chains *via* a hydrogen bond from the remaining acidic hydrogen of the carboxylic end to one (or both) of the oxygens of the carboxylate end of the anion.[19,25] In fact, many of the shortest O···O hydrogen-bond interactions known have been observed within chains of dicarboxylate anions.[26a,b] This pronounced (and well-established) tendency of monovalent anions of dicarboxylic acids to form infinite chains throughout a solid provides an important design element in this project. However, we also need to be able to control the assembly of these one-dimensional aggregates into two and, finally, into three dimensions before we can claim a significant degree of success.

In our search for a potentially suitable anionic building block, we opted for enantiomerically pure L-malic acid as a starting point.[26c] Malic acid, a chiral dicarboxylic acid, was chosen for this program since its monovalent anion (with two hydrogen-bond donors and five hydrogen-bond acceptors) has the potential for creating a layered, two-dimensional network through directed, specific, hydrogen-bond interactions.

Firstly, infinite chains can be constructed through the expected head-to-tail hydrogen bond between adjacent, monovalent anions. Secondly, the presence of the hydroxy group (with one hydrogen-bond donor and one acceptor) almost at a right angle to the infinite chain of anions can now be utilized as a means for cross-linking adjacent chains. This idea would be in accordance with another rule-of-thumb observed by Donohue,[27] stating that all available acidic hydrogens in a molecule will be used in hydrogen bonding in the crystal structure of that compound. It is quite possible that the hydroxy group will hydrogen bond to a suitable site on the cation, but a recent study of hydrogen tartrate structures demonstrated that the two hydroxy groups on the monovalent hydrogen tartrate anion almost invariably provided hydrogen-bonded links between adjacent anionic chains.[14] Finally, if the anions do create hydrogen-bonded, 2-D, aggregates, a counterion (with suitable hydrogen-bond donor sites) may then act as a cross-link between adjacent layers, thereby completing the intentional construction of a distinctive, three-dimensional structure.

Unfortunately, the existing literature provides scant structural information on organic hydrogen malates. Malic acid and its salts have often shown a tendency for poor crystal growth,[28] thus explaining the relative shortage of crystallographic data for organic hydrogen malates.[29] To date, X-ray crystallographic studies of resolved hydrogen malates which have provided crystallographic data of sufficient quality (*e.g.*, location of hydrogen atoms, $R = <7.5\%$) only comprise two monovalent cations: $[NH_4]^+$ [30] and Li^+.[31]

In order to investigate our supposition, we have embarked on an extensive synthetic and X-ray crystallographic project with a view to establishing the suitability of hydrogen malate anions as building blocks for two-dimensional aggregates.

We initially chose to incorporate "trivial" cations in order to study hydrogen-bond interactions in the absence of predesigned cavities or complimentary functional groups. The simplicity of the synthetic procedure means that we can quickly prepare a large number of hydrogen L-malate salts, which accelerates the process of identifying compounds that produce crystals of sufficient quality for X-ray single crystal determination. We are currently performing a systematic structural study of related cations within the hydrogen malate framework, an approach which is essential if we are to attain a real understanding of how to control the arrangement of ions within hydrogen-bonded salts.

In this paper, we report the syntheses and X-ray single crystal characterizations of four new salts, 3-hydroxy-6-methylpyridinium hydrogen L-malate (**1**), benzimidazolium hydrogen L-malate (**2**), 3-hydroxypyridinium hydrogen L-malate (**3**), and (2-chlorobenzyl)ammonium hydrogen L-malate (**4**). The four cations were chosen mainly because of the positioning of their hydrogen-bond donors/acceptors. 3-Hydroxypyridine has a donor site and an acceptor/donor site at opposite ends of a rigid spacer, and a similar arrangement is found in 3-hydroxy-6-methylpyridine, but with the extra bulk provided by the methyl group. The (2-chlorobenzyl)ammonium ion should not be able to provide a cross-link between the expected anionic layers, due to the close proximity of its three hydrogen-bond donors, and finally, the benzimidazolium ion combines two donors with a slightly bulkier, rigid frame.

Results

The syntheses of **1**−**4** are described in detail in the Experimental Section, and the relevant X-ray crystallographic information is displayed in Table 1. ORTEP drawings showing numbering schemes and geometries of the ion pairs in **1**−**4** are presented in Figures 1a−d.

(17) (a) Aakeröy, C. B.; Hitchcock, P. B.; Moyle, B. D.; Seddon, K. R. *J. Chem. Soc., Chem. Commun.* **1989**, 1856. (b) Masse, R.; Durif, A. Z. *Kristallogr.* **1990**, *190*, 19.
(18) Pecaut, J.; Le Fur, Y.; Masse, R. *Acta Crystallogr.* **1993**, *B49*, 535.
(19) Leiserowitz, L. *Acta Crystallogr.* **1976**, *B32*, 775.
(20) Bailey, M.; Brown, C. J. *Acta Crystallogr.* **1967**, *22*, 387.
(21) Kryger, L.; Rasmussen, S. E.; Damielsen, J. *Acta Chem. Scand.* **1972**, *26*, 2339.
(22) Housty, J.; Hospital, M. *Acta Crystallogr.* **1965**, *18*, 693.
(23) Etter, M. C.; MacDonald, J. C.; Bernstein, J. *Acta Crystallogr.* **1990**, *B46*, 256.
(24) Etter, M. C. *Acc. Chem. Res.* **1990**, *23*, 120.
(25) MacDonald, J. C. Ph.D. Thesis, University of Minnesota, 1992.
(26) (a) Speakman, J. C. *Structure Bonding* **1972**, *12*, 141. (b) Emsley, J. *Chem. Soc. Rev.* **1980**, *9*, 91. (c) (*S*)-(−)-Malic acid.
(27) Donohue, J. *J. Phys. Chem.* **1952**, *56*, 502.
(28) van der Sluis, P.; Kroon, J. *Acta Crystallogr.* **1985**, *C41*, 956.
(29) Cambridge Structural Database version 5.07 (April 1994). Allen, F. H.; Kennard, O.; Taylor, R. *Acc. Chem. Res.* **1983**, *16*, 46.
(30) Versichel, W.; van de Mieroop, W.; Lenstra, A. T. H. *Acta Crystallogr.* **1978**, *B34*, 2643.
(31) van Havere, W.; Lenstra, A. T. H. *Acta Crystallogr.* **1980**, *B36*, 1483.

Table 1. Data Collection and Refinement for **1**–**4**

	1	**2**	**3**	**4**
emp form	$C_{10}H_{13}NO_6$	$C_{11}H_{12}N_2O_5$	$C_9H_{11}NO_6$	$C_{11}H_{14}ClNO_5$
MW	243.21	252.23	229.19	275.68
crystal size (mm)	0.84 × 0.96 × 0.26	0.61 × 0.72 × 0.25	0.73 × 0.45 × 0.42	0.87 × 0.74 × 0.39
cryst syst	orthorhombic	orthorhombic	orthorhombic	monoclinic
space group	$P2_12_12_1$ (no. 19)	$P2_12_12_1$ (no. 19)	$P2_12_12_1$ (no. 19)	$P2_1$ (no. 4)
a (Å)	7.697(2)	7.526(1)	7.267	6.306(1)
b (Å)	7.753(2)	9.615(1)	7.657(1)	13.902(2)
c (Å)	19.241(4)	15.946(2)	19.272(2)	7.559(1)
β(deg)				107.79(1)
V (Å^3)	1148.2(5)	1153.9(2)	1072.4(2)	631.0(2)
Z	4	4	4	2
D_{calcd} (g cm^{-3})	1.407	1.452	1.420	1.451
F(000)	512	528	480	288
μ(Mo Kα) (mm^{-1})	0.12	0.12	0.121	0.315
T (K)	293	120	293	293
ω scans, 2θ range (deg)	4–50	4–50	4–50	4–50
range of h	−1 to 9	−1 to 8	−1 to 8	−1 to 8
range of k	−1 to 9	−1 to 11	−1 to 9	−1 to 18
range of l	−1 to 22	−1 to 18	−1 to 22	−9 to 9
no. of reflns colld	1674	1646	1589	2038
no. of unique reflns	1514	1495	1413	1620
extinct coeff	0.019(3)		0.019(3)	
data:parameter ratio	9.8	9.2	9.9	9.5
refinement	full-matrix least squares	full-matrix least squares	full-matrix least squares	full-matrix least squares
R/R^2_w (obsd data)	0.0346/0.0979	0.0325/0.0788	0.0308/0.0788	0.0443/0.1162
R/R^2_w (all data)	0.0385/0.1021	0.036/0.0815	0.0361/0.0825	0.0515/0.1261
$\Delta\varrho_{max/min}$ (e Å^{-3})	0.24/−0.23	0.18/−0.28	0.135/−0.199	0.278/−0.212
S	1.081	1.092	1.093	1.075

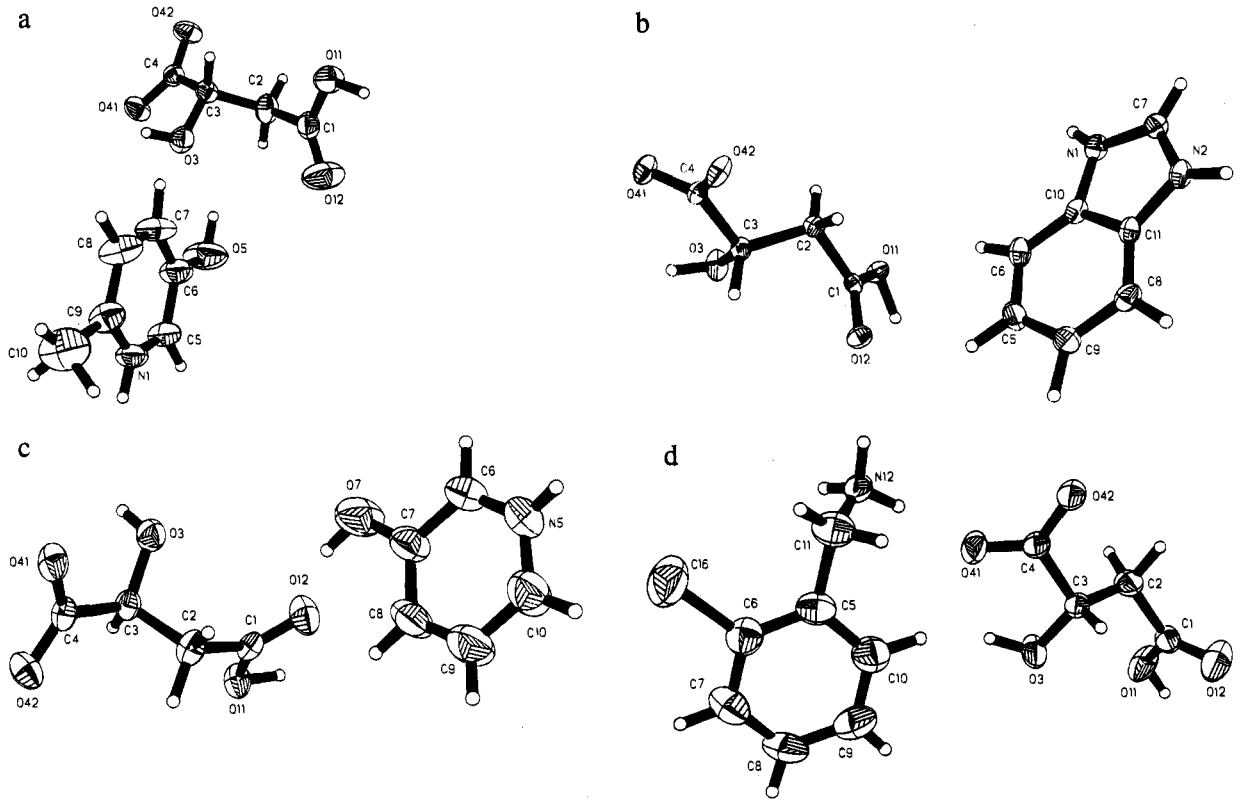

Figure 1. Geometries, thermal ellipsoids (50%), and numbering schemes of the ion pairs in (a) **1**, (b) **2**, (c) **3**, and (d) **4**.

The hydrogen malate anion does have a capacity for considerable conformational freedom, which is also borne out by the structures examined in this study. The C–C–C–C backbone, however, resides in an antiperiplanar form in each case with a torsion angle close to 180° (Table 2). A similar structure was observed in ammonium hydrogen L-malate,[30] although the anion displayed a synclinical configuration in lithium hydrogen L-malate (∠C–C–C–C, −66.6°).[31]

There is ample evidence to suggest that the glycolic acid moiety exhibits a planar conformation in most α-hydroxy carboxylic acids,[32] and such an arrangement is often a result of an intramolecular hydrogen-bond interaction. However, the corresponding moiety of the anion in **1**–**4** deviates significantly from the commonly occurring planar arrangement with values

(32) Stouten, P. F. W.; Kroon-Batenburg, L. M. J.; Kroon, J. *J. Mol. Struct. (THEOCHEM)* **1989**, *200*, 169.

Table 2. Selected Bond Lengths (Å) and Torsion Angles (deg) for Some Hydrogen L-Malates

	1	2	3	4
		Bond Lengths		
C(4)−O(41)	1.257(2)	1.235(3)	1.257(2)	1.235(3)
C(4)−O(42)	1.237(2)	1.275(3)	1.237(2)	1.275(3)
		Torsion Angles		
C(1)−C(2)−C(3)−C(4)	178.47(16)	171.63(19)	175.74(17)	176.19(24)
O(3)−C(3)−C(4)−O(41)	−12.28(27)	3.11(30)	−21.90(26)	2.27(44)
C(2)−C(3)−C(4)−O(41)	107.18(17)	123.56(24)	96.12(20)	125.59(33)

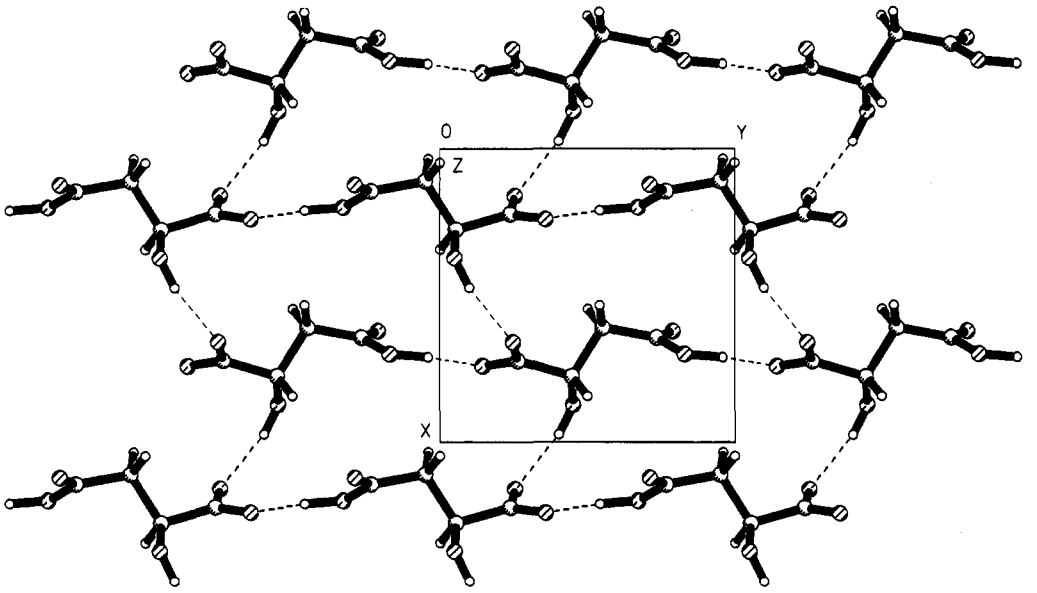

Figure 2. Schematic view of the infinite anionic layer in **1**, with adjacent chains, parallel with *b*, aligned in an antiparallel fashion. Hydrogen bonds are indicated by dotted lines.

of the O(3)−C(3)−C(4)−O(41) torsion angle ranging from −22 to 3° (Table 2) (the oxygen atom at the deprotonated end which makes the smallest torsion angle with O(3) is consistently defined as O(41)). This variation must be attributed to differences in specific hydrogen-bond interactions between the four salts. The arrangement of the carboxylate group with respect to the carbon backbone also exhibits considerable variations, with values for the C(2)−C(3)−C(4)−O(41) torsion angle ranging from approximately 96 to 126° (Table 2). Again, intermolecular hydrogen-bond interactions are likely to significantly influence the geometries of the anions. These observations are in accordance with a theoretical study of L-malic acid[32] which suggests that the relevant rotational barriers are rather small (approximately 15 kJ mol^{-1} for O(3)−C(3)−C(4)−O(41) and 25 kJ mol^{-1} for the C−C−C−C torsion), thereby giving more room for nonbonded forces to influence the final geometry of the anion. Evidence for the strong influence of hydrogen bonding upon the internal geometry of the anion is clearly established through a close examination of the C−O bond distances at the carboxylate end (bonds which, in the absence of noncovalent forces, are expected to be equivalent). For all four salts, there is a significant difference in the bond distance between C(4)−O(41) and C(4)−O(42) (Table 2). In each case, the longer C−O bond involves the oxygen atom which also acts as a hydrogen-bond acceptor in the short, strong, O−H···O interaction (head-to-tail), resulting in infinite anionic chains. Note, also, that either of the two oxygen atoms at the carboxylate end, O(41) or O(42), can participate in the head-to-tail link, O(41) in **1** and **3** and O(42) in **2** and **4**. This provides a good example of the importance of intermolecular hydrogen bonding upon the geometry of individual subunits. Not only are some torsion angles dependent upon hydrogen-bond interactions (which is not very surprising) but even bond lengths can exhibit significant fluctuations as a result of such forces.

Table 3. Geometries of the Hydrogen Bonds in **1**[a]

D−H···A	r(H···A) (Å)	r(D···A) (Å)	∠(D−H···A) (deg)
N1−H(N)···O(41)′	1.870(2)	2.735(2)	177.34(9)
O(5)−H(5)···O(3)	1.910(2)	2.718(2)	147.29(8)
O(11)−H(11)···O(41)″	1.534(2)	2.585(2)	174.53(9)
O(3)−H(3O)···O(41)‴	1.842(2)	2.702(2)	167.60(7)

[a] Symmetry code: (′) $-x$, $1/2 + y$, $1/2 - z$; (″) x, $1 + y$, z; (‴) $-1/2 + x$, $-1/2 - y$, $1 - z$.

The hydrogen L-malate anions in **1** create two-dimensional networks *via* two hydrogen bonds, the expected head-to-tail link between adjacent anions generating a chain parallel with *b*, r[O(11)···O(41)″] 2.585(2) Å, and the cross-link between adjacent chains, r[O(3)···O(42)‴] 2.702(2) Å (Table 3), providing the infinite layer in the *a*−*b* plane (Figure 2). Neighboring chains are aligned in an antiparallel fashion which results in a layer with a slightly puckered appearance when viewed edge on. One potential hydrogen-bond acceptor, O(12), is not used because of a surplus (6:4) of acceptor atoms.

The cation, with hydrogen-bond donors at opposite ends (almost) of a rigid spacer, provides the desired cross-link, parallel to *c*, between adjacent layers through two hydrogen bonds, r[N(1)···O(41)′] 2.735(2) and r[O(5)···O(3)] 2.718(2) Å (Figure 3). The net result is a tightly bound, three-dimensional hydrogen-bonded network. The cation does not display any unexpected structural features.

The anions in **2** also create a two-dimensional network *via* two hydrogen bonds (Table 4). The shorter of the two, r[O(11)···O(42)‴] 2.546(2) Å, creates the head-to-tail chain,

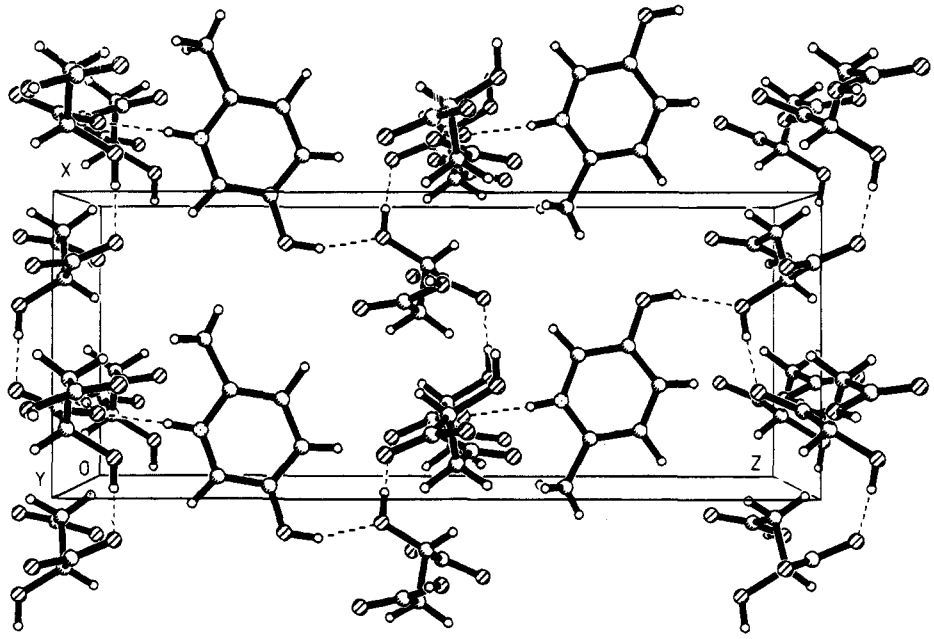

Figure 3. Cross-link, *via* two hydrogen bonds, between adjacent anionic layers in **1** provided by the 3-hydroxy-6-methylpyridinium cation. Only four cations are shown for clarity.

Table 4. Geometries of the Hydrogen Bonds in **2**[a]

D−H···A	r(H···A) (Å)	r(D···A) (Å)	∠(D−H···A) (deg)
N1−H(1)···O(41)′	1.949(3)	2.731(3)	156.76(8)
N(2)−H(2)···O(42)″	1.657(3)	2.683(3)	175.95(9)
O(11)−H(11O)···O(41)‴	1.514(2)	2.546(2)	157.19(9)
O(3)−H(3O)···O(12)⁗	1.980(2)	2.880(2)	164.18(7)

[a] Symmetry code: (′) $-1/2 + x, -1/2 + y, 1 - z$; (″) $-1/2 + x, -1/2 - y, 1 - z$; (‴) $-1 + x, y, z$; (⁗) $1 - x, 1/2 + y, 3/2 - z$.

while the second O−H···O bond, r[O(3)···O(12)⁗] 2.880(2) Å, provides the cross-link between chains to form the desired infinite layer (Figure 4). Furthermore, neighboring chains are again oriented in an antiparallel fashion, thereby producing a puckered layer. In this case, the two hydrogen-bond donors of the benzimidazolium cation are attached to the same anionic layer (Figure 5) and do not provide a cross-link between adjacent layers. This arrangement also means that the aromatic cations are stacked in columns with an inter-ring distance of approximately 3.6 Å.

Similarly, in **3**, the expected hydrogen-bond motif, an infinite layer, is present again and is constructed by the hydrogen L-malate anions *via* two hydrogen bonds, r[O(1)···O(41)″] 2.544(2) Å and r[O(3)···O(42)‴] 2.798(2) Å (Figure 6). The anionic chains, aligned along *b*, are arranged in an antiparallel fashion, producing a slightly puckered layer coinciding with the *a*−*b* plane. The antiparallel arrangement of chains within the layer in the case of **1**−**3** is also reflected by the symmetry of the space group, $P2_12_12_1$.

The cation, with hydrogen-bond sites at opposite (almost) ends of a rigid "spacer", provides the desired cross-link between adjacent layers (Figure 7). This is achieved through two hydrogen bonds, r[N(5)···O(41)′] 2.698(2) Å and r[O(7)···O(12)] 2.623(2) Å (Table 5).

The crystal structure of **4** displays a slightly different arrangement of the anions, but the infinite layer, parallel with the *a*−*c* plane, does remain intact. As previously in **1**−**3**, the anions create a two-dimensional network through two hydrogen bonds, r[O(11)···O(42)‴] 2.559(3) Å and r[O(3)···O(12)″] 2.771(3) Å (Figure 8). Consequently, the infinite chains and the cross-link between adjacent chains *via* the hydroxy group are present within the layer; however, neighboring chains are arranged in a parallel fashion, giving rise to a flat anionic layer. The lower symmetry of this structural feature is also reflected by the space group for **4**, $P2_1$. In addition to the two intermolecular O−H···O bonds between adjacent anions, there is also one intramolecular hydrogen bond in the anion of **4**, r[O(3)···O(41)] 2.608(3) Å. In the sequence **1**−**4**, this anion is the only one with an intramolecular hydrogen bond and it is also the only structure with parallel chains within the anionic layer.

The cation in **4**, (2-chlorobenzyl)ammonium, does not possess hydrogen-bond sites that would allow for a cross-link between adjacent anionic layers. Instead (as expected), the three hydrogen-bond donors, N−H, are all attached to the same side of one layer (Figure 9).

The nearest (nonbonded) neighbor distance to the chlorine atom on the cation is r[Cl···C(11)] 3.760(4) Å, and the chloro substituent does not seem to participate in any specific noncovalent interactions.

Discussion

An examination of four crystal structures of organic hydrogen L-malates, **1**−**4**, has provided considerable support for our premise that hydrogen L-malate anions can be used as a means for creating two-dimensional anionic networks held together by O−H···O hydrogen bonds. This notion is supported by the fact that, while the four cations are connected to the layers in distinctly different ways (due to their particular structural differences), an infinite anionic layer is present in each crystal structure. The appearance of this 2-D aggregate is a consequence of selective, and directional, O−H···O interactions within the anion; the hydrogen malate anion does contain matching hydrogen-bond donors/acceptors. A strong hydrogen-bond donor, −COO(H), consistently links up with the strong hydrogen-bond acceptor, $-COO^-$, to create infinite chains. The hydroxy group then creates a cross-link between adjacent chains by interacting either with the C=O moiety, as in **2** and **4**, or with the remaining oxygen atom at the carboxylate end, as in **1** and **3**.

Apart from the four structures cited here, the anionic layer also appears in ammonium hydrogen L-malate[30] but not in

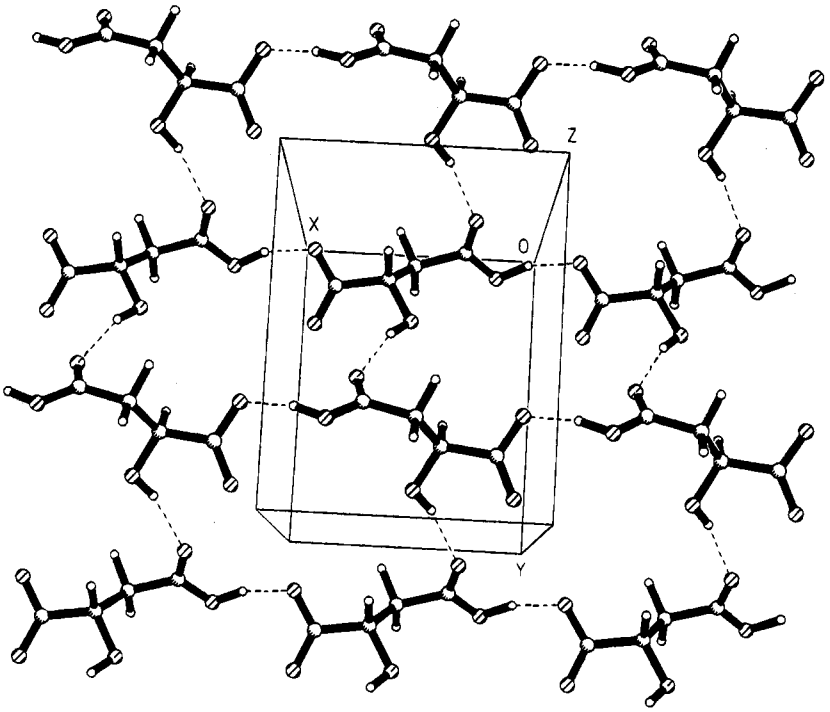

Figure 4. Anionic layer in **2** with adjacent chains aligned in an antiparallel fashion. Hydrogen bonds are indicated by dotted lines.

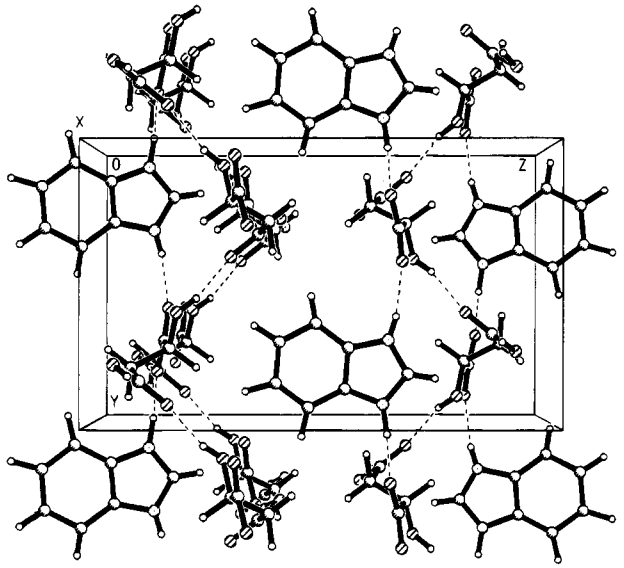

Figure 5. Benzimidazolium cations attached to the puckered anionic layers in **2**.

lithium hydrogen L-malate.[31] Upon the basis of existing structures, it therefore seems probable that the basic structural feature of resolved hydrogen malate salts, represented by the layered anionic scaffolding, will prevail, regardless of the chemical and physical characteristics of the cation, *providing* that the cation is able to supply some hydrogen-bond donor sites. In addition, size may also play a role; if the cation is too small, a layered anionic structure is less plausible, since neighboring, negatively charged, sheets are then forced too close together.

In comparison, the rubidium[33] and cesium[34] salts of hydrogen L-tartrate and ammonium hydrogen D-tartrate[35] all display an anionic 2-D network, whereas the corrresponding lithium and sodium salts have yet to be crystallographically characterized. The small, structurally isotropic, lithium cation (which is also completely lacking hydrogen-bond sites) is unable to provide any (necessary) directional structural support to a potential anionic layer, which results in a complex 3-D network structure for its hydrogen malate salt. (It is also worth noting that the ratios of hydrogen-bond acceptors to hydrogen-bond donors in **1**–**4** and ammonium hydrogen L-malate fall between 1.5 and 0.83, whereas this ratio is 2.5 for the lithium salt.)

The most striking structural difference between the layers in **1**–**4** is the alignment of the anionic chains, antiparallel in **1**–**3** and parallel in **4**. This variation must be controlled by the nature of the cation, but considerably more structural information is required before we can begin to fully rationalize this observation. We do expect that our current systematic crystallographic study of hydrogen malate salts, incorporating a series of closely related (chemically and structurally) counterions, will enable us to identify the specific properties of the cation which give rise to parallel (flat) or antiparallel (puckered) anionic layers.

The presence of the anionic layer (which is the dominating structural motif throughout **1**–**4**) also means that these layers will, if at all possible, mutually adjust to accommodate the hydrogen-bond sites of the cations, thereby "maneuvering" the cations into specific positions within the anionic scaffolding. Consequently, by incorporating a two-dimensional anionic building block into a crystalline salt, we have effectively restricted the conformational and spatial freedom of individual counterions, thereby forcing them into distinctive positions. This approach provides considerable flexibility to the way in which new materials can be constructed, but the realization of this strategy is only possible due to the selectivity and directionality of hydrogen bonds even between ionic species in the solid state.

Another important part of this approach to crystal engineering concerns the ability to recognize and describe patterns and hydrogen-bond preferences displayed by a variety of molecules and ions. The most successful methodology for describing hydrogen-bond patterns has been developed by Etter and coworkers,[23,24] and by applying relatively simple rules in a

(33) Templeton, L. K.; Templeton, D. H. *Acta Crystallogr.* **1989**, *C45*, 675.
(34) Templeton, L. K.; Templeton, D. H. *Acta Crystallogr.* **1978**, *C34*, 368.
(35) Kroon, J.; Duisenberg, A. J. M.; Peerdeman, A. F. *Acta Crystallogr.* **1984**, *C40*, 645.

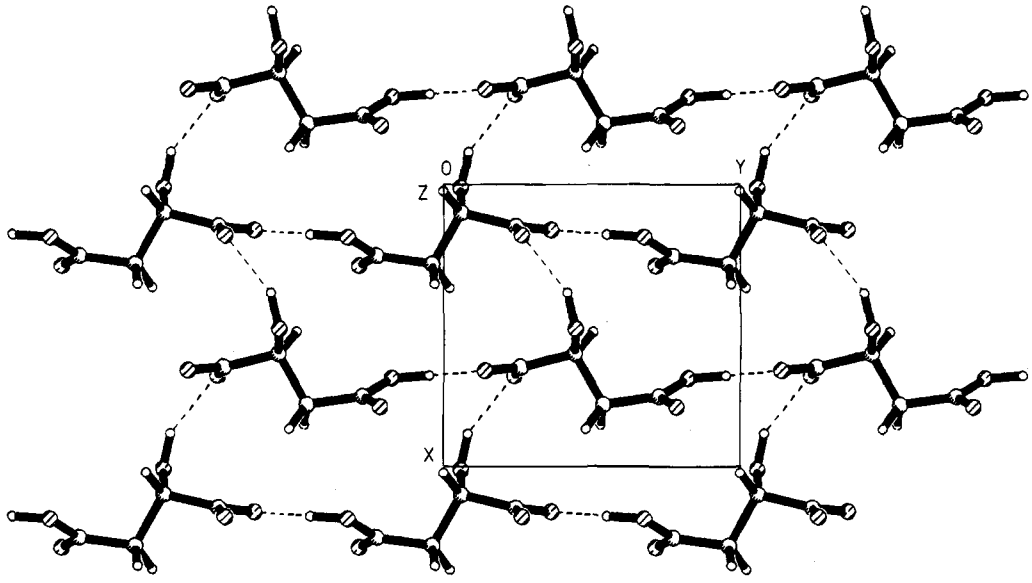

Figure 6. Two-dimensional anionic network in **3**, parallel with the $a-b$ plane.

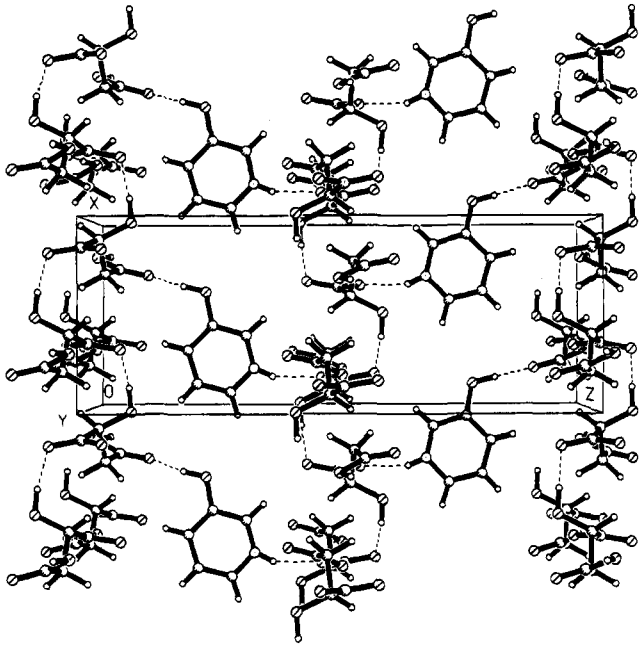

Figure 7. Adjacent anionic layers cross-linked by the 3-hydroxypyridinium cation *via* two hydrogen bonds (dotted lines).

Table 5. Geometries of the Hydrogen Bonds in **3**[a]

D−H···A (Å)	r(H···A) (Å)	r(D···A) (Å)	∠(D−H···A) (deg)
N5−H(5)···O(41)′	1.930(2)	2.698(2)	155.91(8)
O(7)−H(7)···O(12)	1.783(2)	2.623(2)	151.35(10)
O(1)−H(11)···O(41)″	1.497(2)	2.544(2)	172.20(7)
O(3)−H(3O)···O(42)‴	1.919(2)	2.798(2)	152.98(8)

[a] Symmetry code: (′) $1-x$, $1/2-y$, $1/2-z$; (″) x, $y-1$, z; (‴) $x+1/2$, $3/2-y$, $-z$.

systematic fashion, they have been able to identify and classify existing hydrogen-bond motifs in a wide range of compounds. Such an approach, which acknowledges the importance of, and facilitates the recognition of, structural patterns, may play an important role in further developments of crystal engineering. We have chosen to characterize the hydrogen-bond patterns within these anionic networks with a slightly modified descriptor,[14] based around the Etter terminology. This descriptor, which is intended specifically for layered aggregates, provides a

Table 6. Geometries of the Hydrogen Bonds in **4**[a]

D−H···A	r(H···A) (Å)	r(D···A) (Å)	∠(D−H···A) (deg)
N12−H(122)···O(3)′	2.053(3)	2.884(3)	155.14(14)
N12−H(122)···O(41)	1.881(3)	2.793(3)	176.50(12)
N12−H(123)···O(42)″	1.957(3)	2.814(3)	168.55(9)
O(11)−H(11O)···O(42)‴	1.719(3)	2.559*3)	178.49(15)
O(3)−H(3O)···O(12)″	2.177(3)	2.771(3)	119.27(9)
O(3)−H(O3)···O(41)	2.013(3)	2.608(3)	118.71(10)

[a] Symmetry code: (′) x, y, $1+z$; (″) $x-1$, y, z; (‴) x, y, $z-1$.

concise summary of these layers in terms of the number, and size, of "holes" in each 2-D network. The similarity of the overall shape and hydrogen-bond connectivity for these four layers is reflected by the fact that they can all be represented as $N_{2\text{-}D} = L\{R_4^4(22)\}$.[36] The interpretation of this is that every structure, **1**−**4**, contains one unique hydrogen-bonded ring within the anionic network and each ring comprises four hydrogen-bond donors, four acceptors, and 22 atoms in the ring.

Having established the existence of an, ostensibly, reliable 2-D, anionic, building block, the next phase will encompass both the incorporation of this scaffolding as a specific design element in new materials and an examination of how far this motif can be "stretched". Will it be possible to make controlled modifications to the physical properties of a sequence of crystals if the interlayer spacing is changed by a precise distance (if, indeed, this is at all achievable)? How far will the hydrogen malate layers allow themselves to be pushed apart (or, indeed, how close together) before the structure collapses?

Finally, although the anionic layer is present in **1**−**4**, its detailed structure (*e.g.*, alignment of chains and the size of "holes" within the net) can be influenced by the nature of the cation. In addition, once the layer has been established, the space between adjacent layers, and the way in which they are connected, will be determined by the (physico)chemical characteristics of the cation. We may, thus, be able to make controlled adjustments to the distance between layers by employing rigid "spacers" of varying length. These "spacers"

(36) The descriptor employed here for classifying two-dimensional aggregates is $N_{2\text{-}D} = L\{R_d^a(n)'R_d^a(n)''R_d^a(n)\cdots\}$, where $N_{2\text{-}D}$ indicates a two-dimensional network, L specifies it to be of a layered, or sheet-like type. The layer consists of hydrogen-bonded rings, R, where n refers to the number of atoms in a ring and d and a are the number of hydrogen-bond donors and acceptors participating in the ring.

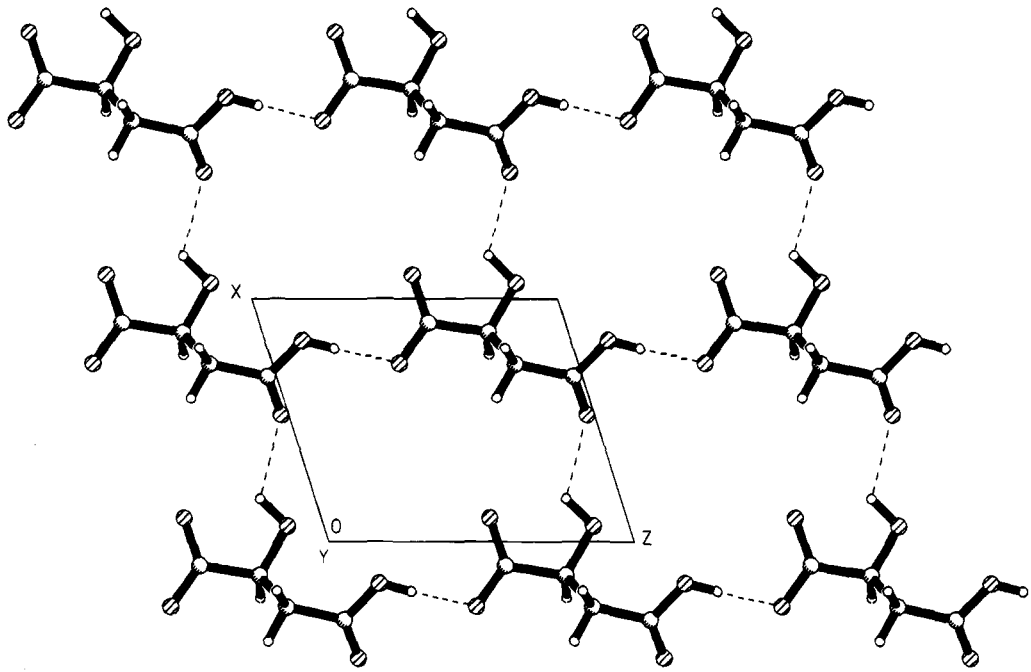

Figure 8. Schematic view of the two-dimensional anionic network in **4**, generated by two hydrogen bonds (dotted lines).

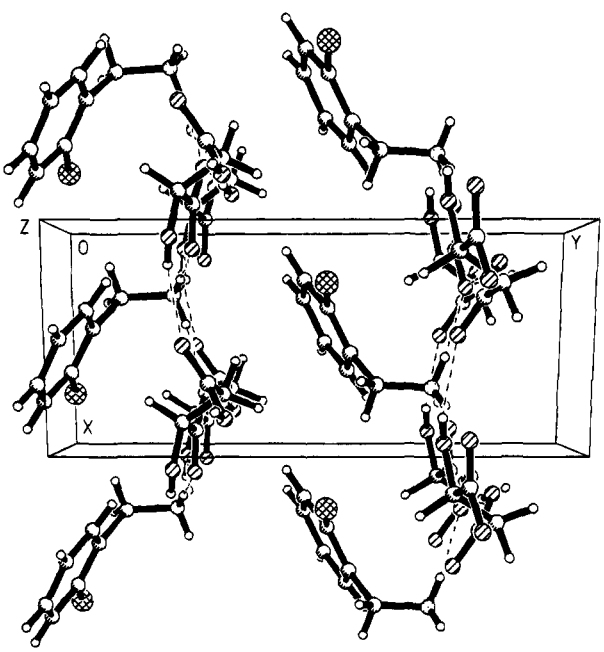

Figure 9. Packing diagram of the structure of **4**. Layers of cations and anions are shown, with each cation attached to only one layer.

can be equipped either with suitable hydrogen-bond sites at opposite ends of the molecule in order to cross-link adjacent layers or with hydrogen-bond sites at one end of the molecule which will serve to "anchor" the spacer to one side of the layer.

Summary

We have established that hydrogen L-malate anions can be used as a means of providing structural consistency and rigidity in crystalline solids by creating anionic layers, held together by two hydrogen bonds. Since these two-dimensional networks can be treated as reliable and extended structural building blocks, it may be possible to induce small (and predictable) structural changes within a family of novel materials by incorporating a sequence of cations with slightly varied geometric features. Since we are starting with an enantiomerically pure material, the chirality of the anion guarantees a non-centrosymmetric space group and will therefore increase the possibilities of producing new polar materials with nonlinear optical or ferroelectric properties. In addition, the inherent anisotropy of such layered materials may also form a basis for new magnetic materials (especially *via* incorporation of cationic transition-metal complexes).

Experimental Section

3-Hydroxy-6-methylpyridinium Hydrogen L-Malate (1). An aqueous solution of 3-hydroxy-6-methylpyridine (1.16 g, 10.6 mmol) was added to an ethanolic solution of L-malic acid (1.45 g, 10.8 mmol). The resulting mixture was left to evaporate to near dryness at ambient temperature. The white solid was filtered off and recrystallized twice from water to produce colorless hexagonal crystals, mp 112–113 °C. Anal. Calcd. for $C_{10}H_{13}NO_6$: C, 48.98; H, 6.17; N, 5.71. Found: C, 48.6; H, 6.1; N, 5.6.

Benzimidazolium Hydrogen L-Malate (2). Benzimidazole (0.34 g, 2.88 mmol) was dissolved in ethanol (5 cm^3) and added to an aqueous solution of L-malic acid (2.92×10^{-3} M). Platelike, colorless, crystals were formed upon evaporation of the solvents, mp 109–110 °C. Anal. Calcd for $C_{11}H_{12}N_2O_5$: C, 52.38; H, 4.76; N, 11.11. Found: C, 51.6; H, 4.9; N, 10.9.

3-Hydroxypyridinium Hydrogen L-Malate (3). 3-Hydroxypyridine (0.35 g, 3.68 mmol) was dissolved in ethanol (5 cm^3) and added to an aqueous solution of L-malic acid (2.92×10^{-3} M). Slow evaporation of the solvent yielded large platelike, colorless, crystals, mp 87–88 °C. Anal. Calcd for $C_9H_{11}NO_6$; C, 47.17; H, 4.84; N, 6.11. Found: C, 47.8; H, 4.7; N, 6.4.

(2-Chlorobenzyl)ammonium Hydrogen L-Malate (4). 2-Chlorobenzylamine (0.35 g, 2.50 mmol) was added to a water–ethanol (1:1) solution of L-malic acid (2.92×10^{-3} M). Thin, colorless, needles appeared upon evaporation of the solvents. The product was slowly recrystallized from a water–ethanol (1:1) mixture to produce irregular, colorless crystals, mp 161–162 °C. Anal. Calcd for $C_{11}H_{14}ClNO_5$: C, 47.92; H, 5.12; N, 5.08. Found: C, 47.8; H, 5.1; N, 5.1.

X-ray Crystallography. Crystal data were collected using a Siemens P4 four-circle diffractometer with graphite monochromated Mo Kα radiation.[37] Crystal stabilities were monitored by measuring standard reflections every 100 reflections, and there were no significant variations (<±1%). Cell parameters were obtained from 35 accurately centered reflections in the 2θ range 10–28°. ω scans were employed

for data collection, and Lorentz and polarization corrections were applied. In the cases of **1** and **3**, extinction coefficients were applied. The configuration for the salts was determined by the fact that enantiomerically pure L-malic acid was used as the starting material for all products.

The structures were solved by direct methods, and the non-hydrogen atoms were refined with anisotropic thermal parameters. Hydrogen-atom positions were located from difference Fourier maps, and a riding model with fixed thermal parameters ($B_{iso} = 1.2B_{eq}$ for the atom to which they are bonded) was used for subsequent refinements. The function minimized was $\sum[\omega(|F_o|^2 - |F_c|^2)]$ with reflection weights $\omega^{-1} = [\sigma^2 |F_o|^2 + (g_1P)^2 + (g_2P)]$, where $P = [\max|F_o|^2 + 2|F_c|^2]/3$. The SHELXTL PC and SHELXL-93 packages were used for data reduction and structure solution and refinement.[38]

Supplementary Material Available: Tables of atomic coordinates, isotropic and anisotropic displacement coefficients, and bond lengths and angles (16 pages); structure factor tables (16 pages). This material is contained in many libraries on microfiche, immediately follows this article in the microfilm version of the journal, and can be ordered from the ACS; see any current masthead page for ordering information.

(37) In order to verify that the chosen single crystal was representative of the bulk material, the X-ray powder diffraction pattern was simulated from the single crystal data (using the CERIUS 3.2 package) and compared with the experimental X-ray powder pattern recorded on the bulk sample. The match between simulated and experimental patterns demonstrated that only one structural form of **1**−**4** was present in each case.

(38) Sheldrick, G. M. SHELXL-93, University of Göttingen.